Strain and compositional fluctuations in Al0.81In0.19N/GaN heterostructures

V. Portz, M. Schnedler, M. Duchamp, F.-M. Hsiao, H. Eisele, J.-F. Carlin, R. Butté, N. Grandjean, R. E. Dunin-Borkowski, and Ph. Ebert

---

Articles you may be interested in

Elimination of columnar microstructure in N-face InAlN, lattice-matched to GaN, grown by plasma-assisted molecular beam epitaxy in the N-rich regime
Appl. Phys. Lett. **104**, 072107 (2014); 10.1063/1.4866435

Ultrathin InAlN/GaN heterostructures on sapphire for high on/off current ratio high electron mobility transistors
J. Appl. Phys. **113**, 214503 (2013); 10.1063/1.4808260

Calculations for the band lineup of strained In x Ga 1 − x N / GaN quantum wells: Effects of strain on the band offsets
J. Appl. Phys. **105**, 046101 (2009); 10.1063/1.3066716

Strain distribution of thin InN epilayers grown on (0001) GaN templates by molecular beam epitaxy
Appl. Phys. Lett. **90**, 061920 (2007); 10.1063/1.2470496

Influence of alloy composition and interlayer thickness on twist and tilt mosaic in Al x Ga 1−x N/AlN/GaN heterostructures
Appl. Phys. Lett. **83**, 5434 (2003); 10.1063/1.1637717

Strain and compositional fluctuations in Al$_{0.81}$In$_{0.19}$N/GaN heterostructures

V. Portz,[1] M. Schnedler,[1] M. Duchamp,[1,2] F.-M. Hsiao,[1,3] H. Eisele,[4] J.-F. Carlin,[5] R. Butté,[5]
N. Grandjean,[5] R. E. Dunin-Borkowski,[1,2] and Ph. Ebert[1,a)]

[1]Peter Grünberg Institut, Forschungszentrum Jülich GmbH, 52425 Jülich, Germany
[2]Ernst Ruska-Centrum, Forschungszentrum Jülich GmbH, 52425 Jülich, Germany
[3]Department of Physics, National Sun Yat-sen University, Kaohsiung 80424, Taiwan
[4]Institut für Festkörperphysik, Technische Universität Berlin, Hardenbergstraße 36, 10623 Berlin, Germany
[5]Institute of Physics, Ecole Polytechnique Fédérale de Lausanne, 1015 Lausanne, Switzerland

The strain and compositional fluctuations of nearly lattice-matched Al$_{0.81}$In$_{0.19}$N/GaN heterostructures are investigated by cross-sectional scanning tunneling microscopy and selected area electron diffraction measurements in scanning electron transmission microscopy. The presence of strain induces height modulations governed by different roughness components at the cleavage surfaces. The surface height modulations are compatible with a relaxation of alternatingly compressive and tensile strained domains, indicating compositional fluctuations. Changes of the *a* lattice constant are traced to interface misfit edge dislocations. The dislocations induce steps increasing the roughness within the Al$_{0.81}$In$_{0.19}$N layers. *Published by AIP Publishing.*
[http://dx.doi.org/10.1063/1.4963184]

The Al$_{1-x}$In$_x$N alloy attracted increasing interest for optoelectronic and electronic applications due to a substantial refractive index contrast to GaN combined with the possibility to grow lattice-matched layers on GaN.[1,2] Thus, the formation of cracks and additional threading dislocations may be avoided. Furthermore, the band gap of Al$_{1-x}$In$_x$N can be tuned over an exceptionally wide range, from 0.7 eV (InN) to 6.2 eV (AlN), by adjusting the indium (In) composition.[3,4] Therefore, Al$_{1-x}$In$_x$N/GaN is the material of choice for the realization of high reflectivity III-nitride distributed Bragg reflectors.[2,5,6]

The quality of such Al$_{1-x}$In$_x$N materials depends, however, sensitively on strain and compositional fluctuations. For example, tensile strain occurring at GaN/Al$_{1-x}$In$_x$N interfaces was attributed to In surface segregation, causing the formation of dislocations.[7] Also the large Stokes shifts of up to 1 eV measured on Al$_{1-x}$In$_x$N were attributed to fluctuations of the In content.[2,8–11] Even small In fluctuations affect the local band gap, the photoluminescence, and carrier scattering, hence changing the properties of quantum heterostructures or high electron mobility transistors (HEMTs).[2,10] It is therefore of high importance to identify and control strain and In composition fluctuations in Al$_{1-x}$In$_x$N.

In this letter, we determine fluctuations of the lattice constant and the roughness of cross-sectional cleavage surfaces of nearly lattice-matched Al$_{0.81}$In$_{0.19}$N/GaN heterostructures by scanning tunneling microscopy (STM) and selected area electron diffraction (SAED) in scanning transmission electron microscopy (STEM). The height modulation at the $(10\bar{1}0)$ cleavage surface is assigned, on the one hand, to strain relaxation of alternating compressive and tensile domains, attributed to compositional fluctuations, and on the other hand to interface misfit edge dislocations.

We investigated a heterostructure consisting of five repetitions of 31 nm thick Al$_{0.81}$In$_{0.19}$N layers separated by 105 nm thick GaN interlayers grown by metal organic

vapour phase epitaxy (MOVPE) at a surface temperature of 740 °C. The heterostructure is deposited on a 500 nm thick GaN buffer layer grown on *c*-plane free-standing GaN and capped by a 1 μm thick GaN layer. The layer thicknesses and the In content of 19.15% were determined by high resolution X-ray diffraction. At this In content, the Al$_{0.81}$In$_{0.19}$N layers are almost lattice-matched to GaN along the *a* direction.[7]

For cross-sectional STM measurements, the samples were contacted by Au and cleaved in ultrahigh vacuum ($p < 10^{-8}$ Pa) to obtain clean $(10\bar{1}0)$ surfaces. The cleavage surfaces, investigated by STM without interruption of the vacuum, provide a cross-sectional view of the complete heterostructure [Fig. 1(a)]. Fig. 1(c) shows a magnification, in which one can identify from bottom to top: the GaN substrate, the GaN buffer, the five pairs of Al$_{0.81}$In$_{0.19}$N/GaN layers, and the GaN cap. The Al$_{0.81}$In$_{0.19}$N layers appear brighter than the surrounding GaN. In addition, broad height modulations are present, giving rise to dark and bright stripes extending diagonally through the complete heterostructure [see white arrows in Fig. 1(a)]. These height modulations are typical for strained materials relaxing at the cleavage or free surface.[12–14] At larger magnifications, additional contrast fluctuations on a smaller length scale are discernable in the Al$_{0.81}$In$_{0.19}$N layers.

In order to identify the different contributions to the contrast fluctuations, height profiles are measured along the $[1\bar{2}10]$ direction within each layer. Two examples, for the first Al$_{0.81}$In$_{0.19}$N layer and the upper part of the GaN buffer [see blue and red-white dotted lines in Fig. 1(a)], are shown in Fig. 1(b). They exhibit root mean square (rms) roughnesses of 0.71±0.08 nm and 0.43±0.07 nm, respectively. The main contribution to the roughness arises from the broad height modulations marked by white arrows in Fig. 1(a). Additionally, smaller contrast fluctuations are superimposed on the height modulation.

In order to separate the different roughness contributions, we performed a detailed roughness analysis of height profiles for each layer. The profiles with a length of 14 μm

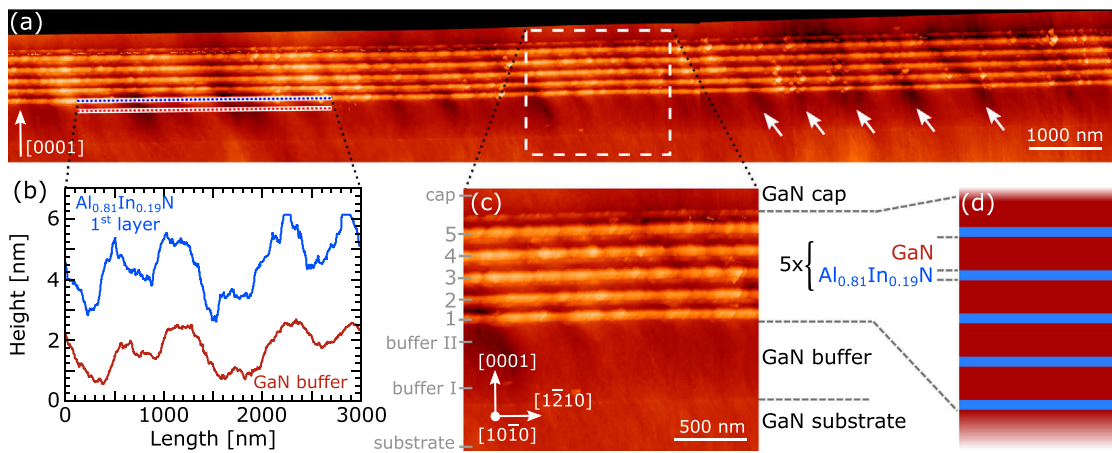a)Electronic mail: p.ebert@fz-juelich.de

FIG. 1. (a) Cross-sectional STM overview image of the $Al_{0.81}In_{0.19}N/GaN$ heterostructure measured at $-4\,V$ and $100\,pA$. The $Al_{0.81}In_{0.19}N$ layers appear brighter than the surrounding GaN. Note the presence of long range contrast fluctuations indicated by the white arrows and additional fluctuations at smaller scale within the $Al_{0.81}In_{0.19}N$ layers. (b) Height profiles measured along the first $Al_{0.81}In_{0.19}N$ layer and the GaN buffer (blue-white and red-white dotted lines in (a), respectively). (c) Magnification of the area in the rectangle in (a). The complete epitaxial structure can be recognized from bottom to top: GaN substrate, GaN buffer, $5\times$ ($31\,nm$ $Al_{0.81}In_{0.19}N/105\,nm$ GaN), and GaN cap. The grey dashes on the left side indicate the positions along the growth direction where a roughness analysis was performed. (d) Schematic of the heterostructure.

were extracted at the spatial positions marked by grey dashes on the left hand side of Fig. 1(c). Because of the large size of the STM image, nonlinear distortions were rectified beforehand to obtain accurate distance measurements.[15] The power spectral density (PSD) is extracted from the height profiles.[16] Figure 2 exemplifies the PSD of the first $Al_{0.81}In_{0.19}N$ layer. The PSDs of all layers exhibit three regions with a roughly exponential decay (linear in the logarithmic scale shown) with different slopes as indicated by the colored dashed lines. At spatial frequencies larger than $0.06\,nm^{-1}$, almost constant PSD values occur (white noise). Hence, the PSD can be best fitted by the sum of three exponential decays shown as grey solid line.

Each exponential decay corresponds in real space to a Lorentzian shaped roughness component, with its specific correlation length c_L and rms roughness R^2.[17,18] c_L is given as the half width at half maximum of the Lorentzian function, while R is given by the maximum of the Lorentzian
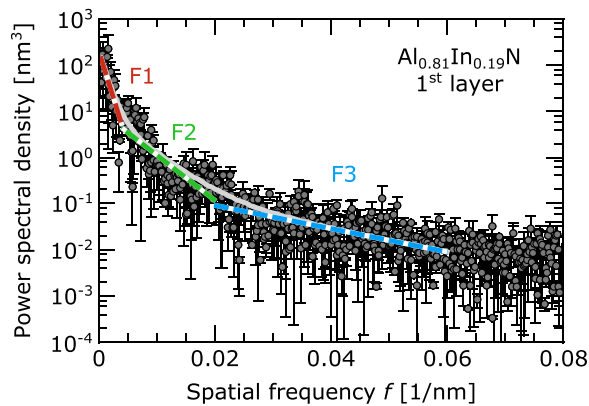
function. By fitting the three exponential decays to the PSD of every layer, we derive for the three frequency ranges the roughness R and correlation length c_L, which are shown in Fig. 3 with the respective line colors as in Fig. 2.

The central result is that the rms roughnesses of all three components are significantly larger within the $Al_{0.81}In_{0.19}N$ layers as compared to the surrounding GaN. The feature labeled F1 has the largest correlation length. This component extends also into the buffer and the cap as indicated by a significantly higher roughness in the buffer close to the first $Al_{0.81}In_{0.19}N$ layer (buffer II position) and in the cap as compared to the substrate and the buffer layers close to the

FIG. 2. Power spectral density vs. spatial frequency f calculated from height profiles measured within the first $Al_{0.81}In_{0.19}N$ layer. The solid grey curve is a fit to the experimental data assuming three different exponential decays with different intensities and correlation lengths. The three exponential decays correspond in real space to three types of features discussed in the text. The dashed red, green, and blue coloured lines show the individual decays and indicate the respective spatial frequency ranges.
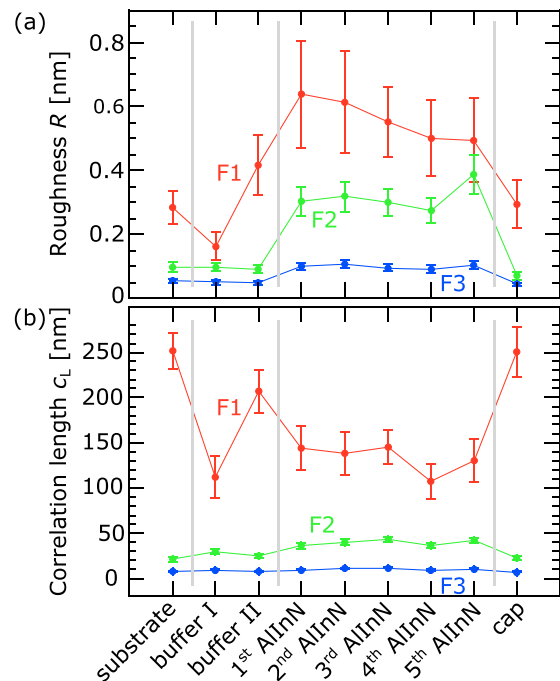

FIG. 3. (a) Roughness R and (b) correlation length c_L extracted from the power spectral densities of the different layers shown according to the growth sequence (horizontal axis) within the $Al_{0.81}In_{0.19}N/GaN$ heterostructure. The three different components to the roughness found for each layer are labeled F1 (red), F2 (green), and F3 (blue).

substrate (buffer I position). The correlation lengths of component F1 $c_{L,F1}$ are 133 ± 11 nm in the $Al_{0.81}In_{0.19}N$ layers and between 100 and 250 nm in the surrounding GaN. This component is directly visible in the STM images as broad height modulations marked by white arrows in Fig. 1(a). They extend slightly diagonally from the buffer II region through all $Al_{0.81}In_{0.19}N$ layers into the cap. Note, the large correlation length with only small rms roughness measured on the substrate is indicative of the typical cleavage surface of unstrained GaN. This effect is not connected to the $Al_{0.81}In_{0.19}N$ layers.

The other two components labeled F2 and F3 are again more intense on the $Al_{0.81}In_{0.19}N$ layers. The average correlation lengths of the $Al_{0.81}In_{0.19}N$ layers are $c_{L,F2} = 39.2 \pm 3.2$ nm and $c_{L,F3} = 10\pm1.1$ nm, respectively. They can be discerned in the STM images as the small contrast features in each $Al_{0.81}In_{0.19}N$ layer.

In order to obtain a deeper insight into the origin of the different roughness components, we prepared cross-sectional STEM specimens by ion beam milling. A final cleaning was performed with low energy Ar$^+$ ion bombardment (0.5 eV) at liquid N_2 temperature using a Fischione Nanomill system. Structural investigations were performed using a FEI Titan STEM equipped with a spherical aberration corrector at the condenser plane. We probed the spatial distribution of the lattice constants using selected area electron diffraction with a beam diameter of 10 nm. Figure 4(b) illustrates an electron diffraction pattern of $Al_{0.81}In_{0.19}N$, which shows the typical reflections of the wurtzite structure along the $[10\bar{1}0]$ zone axis. The peak separations along the reciprocal space directions [0002] and $[1\bar{2}10]$, Δ_c and Δ_a, yield the inverse of the c and a lattice constants, respectively. Figure 4(a) presents the spatial distribution of the obtained local c and a lattice constants in an area covering the GaN buffer
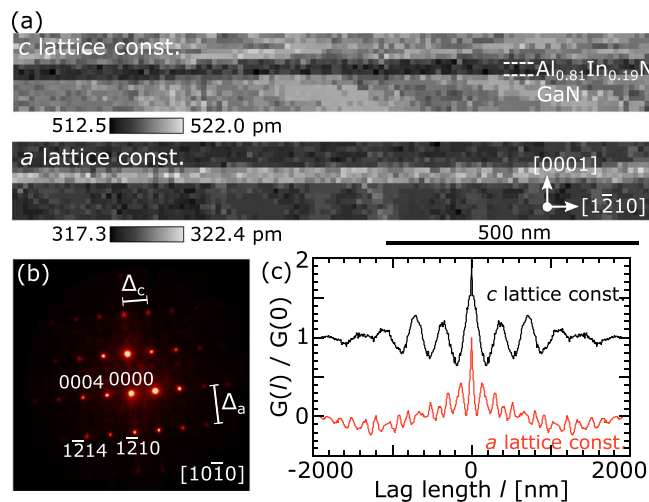
(bottom), the first $Al_{0.81}In_{0.19}N$ layer, and the following GaN interlayer (top). Although the $Al_{0.81}In_{0.19}N$ layers are nominally lattice-matched in the a direction to GaN, Fig. 4(a) shows a clear contrast, i.e., differences in lattice constants. The a and c lattice constants of the $Al_{0.81}In_{0.19}N$ layer deviate from those of GaN by +2 pm and −4 pm, respectively.

Furthermore, extended diagonally oriented stripes can be observed in the c lattice constant while a shorter spatial modulation of the a lattice constant is discernable, both particularly well in the GaN layers and in the respective autocorrelation functions (G(l)/G(0))[16] [Fig. 4(c)]. The wavelengths $2w$ of these modulations were extracted by fitting sine waves to G(l)/G(0). Since the roughness analysis of the STM measurements was performed on the basis of Lorentzian functions, we converted w into the half width at half maximum of the Lorentzian function. This is done by equalizing the separation of adjacent points of inflection of the sine w with that of the Lorentzian function. Hence, the correlation length of the Lorentzian is given as $c_L = \frac{\sqrt{3}}{2}w$ and we obtained c_L values of 147 ± 13 nm and 49 ± 4 nm for the c and a lattice constants, respectively. These values and the shape of the modulations suggest that the F1 and F2 roughness components can be associated with fluctuations of the c and a lattice constants, respectively.

First, we turn to the roughness component F1 appearing as broad height modulations in the STM images. In analogy to strained InGaAsP/InGaP superlattices,[13] the broad height modulations are assigned to strain relaxation. The surface of a homogeneously strained sample would relax in the shape of one large convex curvature in contradiction to our observations. Alternating domains of compressive and tensile strain, however, exhibit a wavy inward and outward relaxation as observed here. This is corroborated by calculations of the lattice relaxation at the cleavage surface using Autodesk Simulation Mechanical 2016. We modeled a $2.4 \times 2.4 \times 10 \mu m^3$ GaN sample with five 30 nm thick layers of $Al_{1-x}In_xN$ separated by 100 nm thick GaN layers. The $Al_{1-x}In_xN$ layers consisted of cuboid domains of $300 \times 300 \times 30 nm^3$ with alternatingly less and more In than the lattice-matched content. This leads to alternating tensile and compressed domains, respectively. The size of the domains was chosen in accordance with the *smallest* distance of 600 nm between adjacent modulation minima [see Fig. 1(a)]. The cleavage surface was set to relax freely.

In order to calculate the strain due to In fluctuations, stress tensors of $Al_{0.81\pm\Delta x}In_{0.19\mp\Delta x}N$, with $0 < \Delta x < 0.19$, are assigned to alternating cuboid domains and calculated using Hooke's law. The out of plane component of the resulting strain for $\Delta x = 0.05$ is illustrated in Fig. 5(a). Blue (red) indicates areas where the sample surface relaxes inward (outward), corresponding to the tensile (compressed) domains. The resulting peak to valley amplitudes and rms roughnesses R of the relaxed surface are shown in Fig. 5(b). They increase linearly with increasing compositional fluctuation, reaching for reasonably expectable In fluctuation values[19] of $\Delta x = 0.05$ roughnesses of 0.24 nm. This R value is, however, too low to explain the observed roughnesses of $R = 0.56 \pm 0.05$ nm. This suggests additional effects. First, calculations of the tunnel current show that electronic effects of the different In compositions result in height changes one

(a)
c lattice const.
- - - - $Al_{0.81}In_{0.19}N$
GaN
512.5 ▮▮▮ 522.0 pm

a lattice const.
[0001]
└─►$[1\bar{2}10]$
317.3 ▮▮▮ 322.4 pm   500 nm

(b) Δ_c
0004 0000
Δ_a
$1\bar{2}14$ $1\bar{2}10$
$[10\bar{1}0]$

(c)
c lattice const.
a lattice const.
G(l) / G(0)
Lag length l / [nm]
-2000   0   2000

FIG. 4. (a) Spatial distribution of the a (lower frame) and c (upper frame) lattice constants of the first $Al_{0.81}In_{0.19}N$ layer and the surrounding GaN determined from selected area electron diffraction patterns measured by STEM in cross-sectional geometry. The $Al_{0.81}In_{0.19}N$ layer exhibits a clear contrast with a lower c and higher a lattice constant with respect to GaN. In addition, a spatial modulation of both lattice constants is visible. (b) Example of an electron diffraction pattern along the $[10\bar{1}0]$ zone axis acquired on the first $Al_{0.81}In_{0.19}N$ layer (electron beam diameter 10 nm). (c) Normalized autocorrelation functions G(l)/G(0) of the spatial distribution of the a (red) and c (black, offset by +1) lattice constants along the $[1\bar{2}10]$ direction within the GaN buffer.
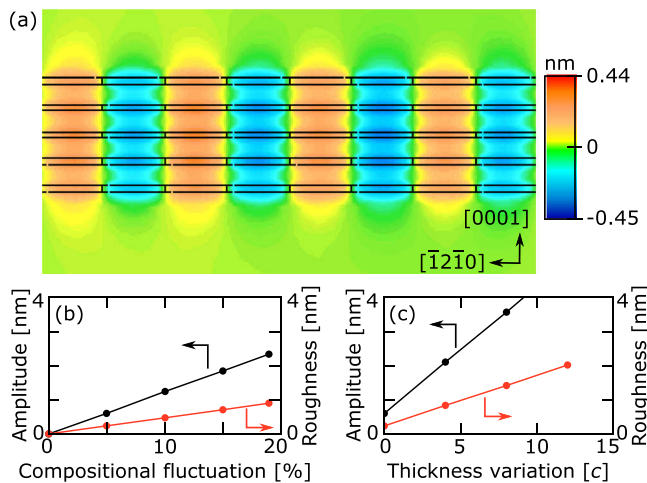
FIG. 5. (a) Color-coded image of the calculated relaxation at the $(10\bar{1}0)$ cleavage surface for five $Al_{1-x}In_xN/GaN(0001)$ pairs embedded in GaN, where each $Al_{1-x}In_xN$ consists of alternating cuboids with an In content of 14% and 24%. (b) Peak to valley amplitude and roughness of $Al_{0.81\pm\Delta x}$ $In_{0.19\mp\Delta x}N$ as a function of the compositional deviation Δx from the nominal In content of 19%. (c) Same, but now for $Al_{0.81\pm0.05}$ $In_{0.19\mp0.05}$ N with in addition different increased or reduced numbers of atomic layers in the compressed and tensile domains, respectively.

order of magnitude smaller and can thus be neglected.[20] Second, it was proposed that the compressed and tensile domains would contain more and less atomic layers than in average, respectively.[21] Such additional layers can be introduced by, e.g., threading dislocations, whose density was reported to be $\sim4\times10^7\,cm^{-2}$ in similarly grown samples,[7] in line with the spatial frequency of dark/bright stripes of the broad height modulation. In addition, compositional fluctuations were related to threading dislocations.[19] Figure 5(c) illustrates the resulting amplitudes and roughnesses of the relaxed surface versus the thickness variation. This effect leads to height modulations in agreement with the experimentally observed roughness component F1. This suggests that the contrast of the F1 component is primarily given by strain relaxation of alternating domains of compositional fluctuations combined with thickness variations. Note, the calculated strain relaxation extends into the surrounding GaN layers, although they have no compositional fluctuations. This is in agreement with the observation.

At this stage, we turn to the roughness component F2. The SAED measurements shown in Fig. 4(a) illustrate that the *a* lattice constant is 0.59% larger in the $Al_{0.81}In_{0.19}N$ layer than in GaN. Such a misfit strain is typically relieved by an interface dislocation network, with an average separation of edge dislocations with an *a*-type Burgers vector of ~54 nm. This value agrees well with the correlation length of the F2 component. Furthermore dislocations with the *a*-type Burgers vector will primarily affect the *a* lattice constant. Hence, we attribute the roughness component F2 to the presence of interface edge dislocations.

The presence of interface edge dislocations is corroborated by the increasing appearance of monoatomic steps within consecutive $Al_{0.81}In_{0.19}N$ layers in analogy to interface edge dislocations at the InN/GaN interface.[22] The steps lead to an increased roughness within the $Al_{0.81}In_{0.19}N$ layers

as compared to the surrounding GaN. Therefore, the roughness component F3 with ~10 nm correlation length can be associated with the atomic steps seen on the surface.

In conclusion, strain and compositional fluctuations of nominally lattice matched $Al_{0.81}In_{0.19}N/GaN$ heterostructures affect the roughness and height modulations at cross-sectional cleavage surfaces and induce local changes of the lattice constants. The strain relaxes at the cleavage surface inducing height modulations, which can be assigned to three roughness components. First, alternatingly compressive and tensile strained domains are found, indicating compositional fluctuations. Second, changes of the *a* lattice constant are traced to interface misfit edge dislocations, which strain primarily the *a* lattice constant and induce surface steps. The latter gives rise to the third component of roughness within the $Al_{0.81}In_{0.19}N$ layers.

[1]J.-F. Carlin and M. Ilegems, Appl. Phys. Lett. **83**, 668 (2003).
[2]R. Butté, J.-F. Carlin, E. Feltin, M. Gonschorek, S. Nicolay, G. Christmann, D. Simeonov, A. Castiglia, J. Dorsaz, H. J. Buehlmann, S. Christopoulos, G. B. H. von Högersthal, A. J. D. Grundy, M. Mosca, C. Pinquier, M. A. Py, F. Demangeot, J. Frandon, P. G. Lagoudakis, J. J. Baumberg, and N. Grandjean, J. Phys. D: Appl. Phys. **40**, 6328 (2007).
[3]J. Wu, W. Walukiewicz, K. M. Yu, J. W. Ager, E. E. Haller, H. Lu, W. J. Schaff, Y. Saito, and Y. Nanishi, Appl. Phys. Lett. **80**, 3967 (2002).
[4]I. Vurgaftman and J. R. Meyer, J. Appl. Phys. **94**, 3675 (2003).
[5]J.-F. Carlin, J. Dorsaz, E. Feltin, R. Butté, N. Grandjean, M. Ilegems, and M. Laügt, Appl. Phys. Lett. **86**, 031107 (2005).
[6]J. Dorsaz, J.-F. Carlin, S. Gradecak, and M. Ilegems, J. Appl. Phys. **97**, 084505 (2005).
[7]G. Cosendey, J.-F. Carlin, N. A. K. Kaufmann, R. Butté, and N. Grandjean, Appl. Phys. Lett. **98**, 181111 (2011).
[8]S. Marcinkevicius, V. Liuolia, D. Billingsley, M. Shatalov, J. Yang, R. Gaska, and M. S. Shur, AIP Adv. **2**, 042148 (2012).
[9]S. Yamaguchi, M. Kariya, S. Nitta, T. Takeuchi, C. Wetzel, H. Amano, and I. Akasaki, Appl. Phys. Lett. **76**, 876 (2000).
[10]V. Liuolia, S. Marcinkevicius, D. Billingsley, M. Shatalov, J. Yang, R. Gaska, and M. S. Shur, Appl. Phys. Lett. **100**, 242104 (2012).
[11]I. Gorczyca, S. P. Łepkowski, T. Suski, N. E. Christensen, and A. Svane, Phys. Rev. B **80**, 075202 (2009).
[12]H. Eisele, O. Flebbe, T. Kalka, and M. Dähne-Prietsch, Surf. Interface Anal. **27**, 537 (1999).
[13]H. Chen, R. M. Feenstra, R. S. Goldman, C. Silfvenius, and G. Landgren, Appl. Phys. Lett. **72**, 1727 (1998).
[14]M. M. J. Treacy and J. M. Gibson, J. Vac. Sci. Technol. B **4**, 1458 (1986).
[15]M. Schnedler, P. H. Weidlich, V. Portz, D. Weber, R. E. Dunin-Borkowski, and Ph. Ebert, Ultramicroscopy **136**, 86 (2014).
[16]J. M. Bennett and L. Mattsson, *Introduction to Surface Roughness and Scattering*, 2nd ed. (Optical Society of America, Washington, DC, 1999).
[17]R. M. Feenstra, D. A. Collins, D. Z.-Y. Ting, M. W. Wang, and T. C. McGill, Phys. Rev. Lett. **72**, 2749 (1994).
[18]N. D. Jäger, K. Urban, E. R. Weber, and Ph. Ebert, Phys. Rev. B **65**, 235302 (2002).
[19]A. Mouti, J.-L. Rouvière, M. Cantoni, J.-F. Carlin, E. Feltin, N. Grandjean, and P. Stadelmann, Phys. Rev. B **83**, 195309 (2011).
[20]R. M. Feenstra, Physica B **273–274**, 796 (1999).
[21]Y. Chen, T. Takeuchi, H. Amano, I. Akasaki, N. Yamada, Y. Kaneko, and S. Y. Wang, Appl. Phys. Lett. **72**, 710 (1998).
[22]H. Eisele, J. Schuppang, M. Schnedler, M. Duchamp, C. Nenstiel, V. Portz, T. Kure, M. Bügler, A. Lenz, M. Dähne, A. Hoffmann, S. Gwo, S. Choi, J. S. Speck, R. E. Dunin-Borkowski, and Ph. Ebert, "Intrinsic electronic properties of high-quality wurtzite InN" (unpublished).